



HAL
open science

The growth of Ti_3SiC_2 coatings onto SiC by reactive chemical vapor deposition using H_2 and $TiCl_4$

H. Fakih, Sylvain Jacques, M.-P. Berthet, F. Bosselet, O. Dezellus, J.-C. Viala

► To cite this version:

H. Fakih, Sylvain Jacques, M.-P. Berthet, F. Bosselet, O. Dezellus, et al.. The growth of Ti_3SiC_2 coatings onto SiC by reactive chemical vapor deposition using H_2 and $TiCl_4$. *Surface and Coatings Technology*, 2006, 201 (6), pp.3748-3755. 10.1016/j.surfcoat.2006.09.040 . hal-04260387

HAL Id: hal-04260387

<https://hal.science/hal-04260387>

Submitted on 26 Oct 2023

HAL is a multi-disciplinary open access archive for the deposit and dissemination of scientific research documents, whether they are published or not. The documents may come from teaching and research institutions in France or abroad, or from public or private research centers.

L'archive ouverte pluridisciplinaire **HAL**, est destinée au dépôt et à la diffusion de documents scientifiques de niveau recherche, publiés ou non, émanant des établissements d'enseignement et de recherche français ou étrangers, des laboratoires publics ou privés.

The growth of Ti_3SiC_2 coatings onto SiC by reactive chemical vapor deposition using H_2 and TiCl_4

H. Fakh, S. Jacques, M.-P. Berthet, F. Bosselet, O. Dezellus, J.-C. Viala

Laboratoire des Multimatériaux et Interfaces – UMR 5615 University of Lyon 1 / CNRS

43 Boulevard du 11 Novembre 1918 F – 69622 Villeurbanne Cedex, France

Address for manuscript correspondence:

Laboratoire des Multimatériaux et Interfaces – UMR 5615 University of Lyon 1 / CNRS

Bâtiment Claude Berthollet, 43, Boulevard du 11 Novembre 1918

F – 69622 Villeurbanne Cedex

France

E-mail address: sylvain.jacques@adm.univ-lyon1.fr

Telephone: +33 (0)4 72 43 13 92

Fax: +33 (0)4 72 44 06 18

Abstract:

$(\text{SiC}/\text{Ti}_3\text{SiC}_2)_n$ multilayered coatings composed of n layers alternately of continuous SiC and Ti_3SiC_2 sub-layers were prepared on carbon substrates. The method consists in depositing SiC by classical chemical vapor deposition (CVD) and then producing a new Ti-containing sub-layer from a reaction between SiC and a H_2/TiCl_4 gaseous mixture by reactive CVD (RCVD), and repeating this sequence n times. In accordance with thermodynamics, this RCVD method produces only pure TiC sub-layers when a low dilution ratio of TiCl_4 in H_2 ($R=[\text{H}_2]/[\text{TiCl}_4]$) is used. With a high R value, the growth of pure Ti_3SiC_2 thin continuous sub-layers from solid-gas reaction is observed for short deposition times. But for long deposition times, the simultaneous growth of additional $\text{Ti}_5\text{Si}_3\text{C}_x$ and TiC sub-layers occurs from solid state diffusion when the initial Ti_3SiC_2 sub-layer thickness exceeds about $1 \mu\text{m}$. In that case, the repeating of the sequence results in the further conversion of the additional phases into new Ti_3SiC_2 sub-layers from solid state reactions involving TiSi_2 as an intermediate phase and SiC.

Keywords: reactive CVD; Ti_3SiC_2 ; multilayer coating; solid-gas reaction; solid state diffusion

1. Introduction

Titanium carbide-silicide Ti_3SiC_2 exhibits unique properties; it is soft and easily machinable, behaves plastically and maintains its strength at high temperature and is resistant to oxidation and thermal shock [1].

As a thin coating, Ti_3SiC_2 has interesting mechanical properties in prospect: it can deform through the formation of kink bands and delamination cracks [2-3]. It is also an excellent electrical and thermal conductor [1] and therefore can be considered for electrical contact layers and connectors at high temperature [4]. In addition, this material exhibits a thermal expansion coefficient around $9 \times 10^{-6}C^{-1}$ over the range 25 - 1200°C [5], which is halfway between SiC (around $4 \times 10^{-6}C^{-1}$) and most metals (Ag: $19 \times 10^{-6}C^{-1}$, Cu: $17 \times 10^{-6}C^{-1}$, Fe: $12 \times 10^{-6}C^{-1}$...). This ternary compound that combines the advantage of both metals and ceramics could be used as an interlayer to join these two dissimilar materials for thermostructural applications.

However, few studies have reported the synthesis of Ti_3SiC_2 films. Thin coatings could be prepared recently by physical vapor deposition [6]. In earliest works, Ti_3SiC_2 coatings were deposited by chemical vapour deposition (CVD) from different gaseous mixtures such as $TiCl_4$ - $SiCl_4$ - CCL_4 - H_2 [7-9] or $TiCl_4$ - $SiCl_4$ - CH_4 - H_2 [10]. CVD allows complex geometrical shape substrates to be coated but these studies highlighted that the deposition of pure Ti_3SiC_2 is difficult.

A previous thermodynamic analysis [11] showed that it is theoretically possible to obtain Ti_3SiC_2 as a single solid phase by reactive CVD (RCVD) through the reaction of $H_2/TiCl_4$ gaseous mixture on solid SiC with a concentration ratio R ($[H_2]/[TiCl_4]$) equal to 4 (Fig. 1.a) if the correct reactant gas/solid ratio is achieved. But, the experimental procedure did not allow the growth of the pure ternary phase. This was attributed to the impossibility of exceeding

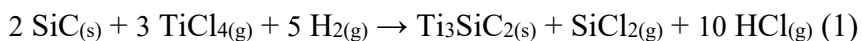
several nanometers in thickness during the first growth of SiC by RCVD (the method used in the previous study) and so to control the gas to solid ratio through matter diffusion [11].

In the present study, we propose to start with a micrometer-thick SiC film deposited by a classical CVD route (in which both silicon and carbon are provided by the gaseous phase) and then to use RCVD for the growth of Ti₃SiC₂ through SiC consumption. For that purpose, we have used a classical low pressure hot wall CVD reactor in which the gaseous pressure and flow are maintained constant during the growth of each layer. As long as solid SiC is available, the gas to solid ratio is therefore controlled by the thickness of the second growing layer, i.e. by the RCVD processing time.

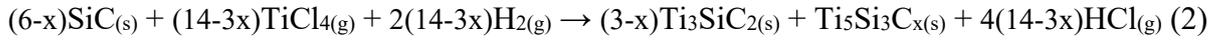
2. Thermodynamic analysis

For the thermodynamic analysis, the computer program used was Gemini 2 and the thermodynamic data were from the Scientific Group Thermodata Europ (Saint Martin d'Hères, France). The temperature was of 1100°C, which is a maximum for our reactor chamber made of silica. The total pressure was set as low as 5 kPa in order to favor coating homogeneity. The calculation details are given in reference [11].

With $R = 4$, Fig. 1a shows that, if the H₂/TiCl₄ gaseous reagent reacts in too large excess with SiC (i.e. more than 4000 moles of TiCl₄ for one mole of SiC), the solid phase obtained at equilibrium is no longer Ti₃SiC₂ but TiC, silicon being vented in the by-product gaseous phase as silicon chlorides: SiCl_p ($p = 2, 3$ and 4). In the case of a very large excess of gaseous reagent, using an R ratio as high as $R = 35$ allows Ti₃SiC₂ to be obtained at equilibrium (Fig. 1b) according to (1):



But it can be also co-deposited with $Ti_5Si_3C_x$ particularly if silicon can not be evacuated in the gaseous phase as $SiCl_2$ (Fig. 1b) according to (2):



where x is a constant value in the range $0 \leq x \leq 1.1$ [12,13].

3. Experimental procedure

3.1. Ti-Si-C layer growth

The coatings were deposited on polycrystalline graphite disks (12 mm in diameter, Ellor 30 from Carbone Lorraine France) placed inside the hot area of a CVD reactor chamber. The CVD apparatus included a horizontal silica tube (30 mm in inner diameter) heated by an electrical resistor furnace. The temperature was 1100°C within the hot area. It was regularly checked between two deposition runs with three Process Temperature Control Rings (type LTH from Ferro Electronic Materials B.V., Uden, The Netherlands) submitted to the same conditions in the reactor as the graphite disks. The total pressure was maintained in the apparatus at a constant value during the deposition of each kind of layer by a vacuum pump through a regulating valve and a pressure gauge. Liquid nitrogen traps permitted the condensation of corrosive by-products such as HCl. Mass flowmeters were used to control the partial gas flow rates of H_2 and CH_3SiCl_3 (MTS).

In each case, a SiC layer was previously deposited by classical CVD from H_2 /MTS to be used as solid carbon and silicon sources for the following Ti-Si-C layer growth. For SiC deposition, the ratio $[H_2]/[MTS]$ was 4, the total gas flow rate was 250 sccm (standard cm^3min^{-1} , i.e. at $P = 101$ kPa and $T = 20^\circ C$) and the total pressure 3 kPa. Then, after evacuation, the $H_2/TiCl_4$ gaseous mixture was introduced in the reactor and the pressure was set at 5 kPa, which

allowed the growth of Ti-Si-C layer(s) by SiC consumption. The titanium tetrachloride vapor was carried by hydrogen through a bubbler at room temperature. The reactant concentration ratio R ($[H_2]/[TiCl_4]$) was adjusted to 4 or 35 by adding pure H_2 with an extra parallel hydrogen feed line and taking into account the value of $TiCl_4$ partial pressure at room temperature. For instance, with a room temperature equal to $20^\circ C$, the $TiCl_4$ partial pressure in the bubbler was 1.28 kPa. The H_2 flow rate was set to 26 sccm through the bubbler and to 290 sccm in the second parallel hydrogen line. With a pressure equal to 5 kPa in the feed lines, the $TiCl_4$ gas flow rate carried out from the bubbler was estimated to 9 sccm, which corresponded to $R = 35$. To obtain $R = 4$, the H_2 flow rate was set to 80 sccm through the bubbler ($TiCl_4$ gas flow rate ≈ 19 sccm) and to 30 sccm in the second parallel hydrogen line. In each case, the deposition sequence (CVD treatment at 3 kPa with H_2/MTS , evacuation, RCVD at 5 kPa with $H_2/TiCl_4$, and evacuation) was repeated several times in order to obtain a total coating thick enough for further characterization. A repetitive deposition sequence was designated as $(S_s/T_t)_n$ where s was the number of minutes used for each previous SiC sub-layer deposition, t the time in minutes chosen for each RCVD reaction with $H_2/TiCl_4$ and n the total number of repeated sequences.

3.2. Characterization

The coated disk surfaces were characterized by X-ray diffraction (XRD: X'Pert Pro MPD from Panalytical, equipped with an X'Celerator detector monochromator, $CuK\alpha$ radiation, Almelo, The Netherlands). Then, the coated graphite disks were broken and the fracture surfaces of the coatings were observed with a scanning electron microscope (SEM: S800 from Hitachi, Tokyo, Japan). With sufficiently thick enough sub-layers (i.e. above $1 \mu m$), cross section composition profiles were determined by electron probe micro-analysis (EPMA: CAMEBAX from CAMECA, Courbevoie, France). EPMA was operated under an accelerating

voltage of 10 kV. After background subtraction, the counting rates obtained for Si and Ti were referred to those recorded under the same conditions on pure and freshly polished standards. After correction for atomic number, absorption and fluorescence, the Si and Ti contents, in percent, were obtained within an error bar not higher than 1 at.%. The carbon content was obtained by subtracting the Ti and Si contents to 100%.

Transmission electron microscopy (TEM) was used (TOPCON 002B, Tokyo, Japan) for thin sub-layers utilizing bright field (BF) and selected area electron diffraction (SAED) techniques. The microscope was equipped with a Kevex energy dispersive spectroscopy (EDS) device for chemical analysis. The chosen spot size for EDS was 56 nm. Only titanium and silicon were considered in the coating analysis (not carbon). Quantitative composition measurements were obtained using the standard Cliff-Lorimer equation. The relative elemental concentration (C_{Ti} and C_{Si}) are related to the measured X-ray peak surfaces above background (S_{Ti} and S_{Si} , respectively) by $C_{Ti}/C_{Si} = k_{SiTi} S_{Si}/S_{Ti}$, where k_{SiTi} is the sensitivity or k-factor. The value of k_{TiSi} was determined from Ti_3SiC_2 grains identified first by SAED in the samples. Ti_3SiC_2 is indeed known as a stoichiometric compound and can serve as a standard. To obtain cross sections for TEM, two pieces of broken coated graphite disks were stuck together with an epoxy resin (Micro-Measurements-Wishay adhesive, Reference M-Bond 610) and mechanically thinned. The thin sheets were then ion-milled (GATAN PIPS, USA) until the electron transparency.

4. Results

4.1. Experimental RCVD with $R = 4$

Figs. 2 and 3 show that a 240 minutes long treatment of a SiC layer by a H₂+TiCl₄ gaseous mixture with a molar ratio H₂/TiCl₄ = 4 (R = 4) results in the growth of a TiC coating of about 3 μm in thickness. Fig. 4 shows the SEM observation of a multilayered coating obtained with shorter treatments. SAED patterns confirm that these RCVD treatments of SiC layers lead also to the formation of pure titanium carbide (Fig. 5). Furthermore, the presence of pores can be noticed in the first one-third part of the TiC layers near the previously deposited SiC layer (Figs. 4 and 5).

Fig. 6 presents the change of the TiC layer thickness versus the duration of the treatment which can be interpolated by a parabolic curve (square root of time) except for the last point at 240 minutes.

4.2. RCVD with R = 35

4.2.1 "Thick layers"

As shown by the thermodynamic analysis, a way to favor the formation of Ti₃SiC₂ by RCVD is to increase the R ratio by dilution in hydrogen. A first multilayered coating was deposited with R = 35 by following three sequences: (S_{60°}/T_{90°})₃. The XRD pattern presented in Fig. 7 reveals the presence of five phases in the multilayered film: SiC, TiC, Ti₃SiC₂, TiSi₂ and Ti₅Si₃C_x. EPMA coupled with SEM observation allows the different phases to be localized across the coating (Fig. 8). As a general trend, the coating consists of a succession of continuous single-phased sub-layers. But surprisingly, even though the three CVD sequences were identical, the three resulting sub-layer sequences found in the whole coating are different from each other. From the carbon disk substrate surface, the coating (about 30 μm thick)) can be described as follow: The first sequence is made of one SiC sub-layer covered with a Ti₃SiC₂ then with a TiSi₂ thin sub-layer (about 1 μm) and then with a last sub-layer of global composition Ti_x-Si_y-C_z that is likely to contain a mixture of TiC and Ti₃SiC₂. The second

sequence is similar to the first one but here the last sub-layer clearly corresponds to Ti_3SiC_2 . The third sequence is quite different from the others: after the SiC sub-layer, a thin TiC sub-layer (about 1 μm in thickness) is first observed before the Ti_3SiC_2 sub-layer. Then the sequence ends with a thick (about 4 μm) $\text{Ti}_5\text{Si}_3\text{C}_x$ sub-layer. Each Ti_3SiC_2 sub-layer detected in the coating is about 2-3 μm thick.

A second multilayered coating was deposited with $R = 35$ but, in this case, the duration chosen for the $\text{SiC}_{(s)} + \text{H}_2/\text{TiCl}_{4(g)}$ RCVD reaction was divided by three: $(\text{S}_{30}/\text{T}_{30})_6$. SEM observation confirms the presence of the six (SiC/Ti-Si-C) bi-layers in the coating (Fig. 9). The corresponding XRD pattern is similar to the previous one except for the TiC phase that was not detected (Fig. 10). A TEM observation performed in the area of sub-layer $n^\circ 5$ reveals the presence of Ti_3SiC_2 crystals (Fig. 11). The total coating thickness is 35 μm but here the thickness of each sub-layer is barely enough for EPMA analysis. So, Si and Ti EDS composition measurements were performed in the TEM on the Ti-Si-C sub-layers $n^\circ 2$, $n^\circ 5$ and $n^\circ 6$ of the thin foil (Fig. 12). This multilayer is quite similar to $(\text{S}_{60}/\text{T}_{90})_3$. Roughly, Ti-Si-C sub-layer $n^\circ 2$ is only made of Ti_3SiC_2 , Ti-Si-C sub-layer $n^\circ 5$ is made of three sub-layers: $\text{Ti}_3\text{SiC}_2/\text{TiSi}_2/\text{Ti}_3\text{SiC}_2$, and the last Ti-Si-C sub-layer is made of two sub-layers: $\text{Ti}_3\text{SiC}_2/\text{Ti}_5\text{Si}_3\text{C}_x$.

4.2.2 "Thin layers"

By reducing more the duration of each deposition sequence, it is possible to obtain submicrometer thin sub-layers as shown in Fig. 13 for $(\text{S}_{10}/\text{T}_{10})_n$ and $(\text{S}_3/\text{T}_3)_n$. In both cases, the XRD patterns only reveal the presence of SiC and especially Ti_3SiC_2 (Fig. 14). In that case, the formation of TiC, $\text{Ti}_5\text{Si}_3\text{C}_x$ and TiSi_2 is avoided and the resulting deposited film is a $(\text{SiC}/\text{Ti}_3\text{SiC}_2)_n$ multilayered coating. It is important to note that from SEM observations, the Ti_3SiC_2 coatings are characterized by plate-like microstructure with grains oriented perpendicular to the substrate surface. This orientation is confirmed by XRD: the $\{008\}$ peak is missing whereas the $\{110\}$ reflection appears stronger than for a calculated powder

diffraction pattern, which indicates that the basal crystallographic planes are oriented perpendicular to the substrate [14]. This result is similar to the previous CVD studies [7-10]

Discussion

The use of different durations for the RCVD treatments allows the relationship between spatial and time sequence to be drawn. With $R = 35$, the rapid growth of pure Ti_3SiC_2 is first observed at the very beginning of the treatment. As long as the treatment duration t does not exceed a critical time denoted as t_{crit} ($t < t_{crit}$, with $10 \text{ min} < t_{crit}' < 30 \text{ min}$), the pure Ti_3SiC_2 layer still grows but at a reduced rate: $1.1 \mu\text{m}$ thick in 3 minutes to only $1.3 \mu\text{m}$ thick in 10 minutes. Then, the very last unit of each multi-layered coating (the one not covered by a new SiC film) must be considered to describe the spatiotemporal growth, i.e. the sixth Ti-Si-C layer in $(S_{30}/T_{30})_6$ and the third one in $(S_{60}/T_{90})_3$. For $t > t_{crit}$, a second layer made of $Ti_5Si_3C_x$ grows at a fast rate: $1.9 \mu\text{m}$ thick in 30 minutes and $6.0 \mu\text{m}$ thick in 90 minutes. At the same time, the first Ti_3SiC_2 sub-layer located near the previously deposited SiC still grows very slowly ($1.7 \mu\text{m}$ thick in 30 minutes and $2.8 \mu\text{m}$ thick in 90 minutes). For a reaction time longer than 30 minutes, a third and thin TiC sub-layer also develops between SiC and Ti_3SiC_2 .

These results tend to show that a one step growth of a pure Ti_3SiC_2 layer thicker than $1.5 \mu\text{m}$ is impossible by RCVD. A way to circumvent this limit and obtain a thick pure Ti_3SiC_2 film should be to repeat short SiC/ Ti_3SiC_2 coating sequences by reducing each SiC sub-layer deposition duration till it is totally consumed, i.e. by realizing $(S_s/T_t)_n$ with $t \leq t_{crit}$ and $s < t$. Experiments are planned to check up on that assumption..

For "thick" Ti-Si-C sub-layers prepared with $t > t_{crit}$, if a new SiC film is deposited on the three-phased $TiC/Ti_3SiC_2/Ti_5Si_3C_x$ coating, two new solid state reactions can develop consistently with the Ti-Si-C phases diagram [11,15-17]. On the one hand, SiC reacts with

$\text{Ti}_5\text{Si}_3\text{C}_x$ to form Ti_3SiC_2 and TiSi_2 . On the other hand, the TiC thin layer formed onto SiC is slowly converted into Ti_3SiC_2 by reaction with $\text{Ti}_5\text{Si}_3\text{C}_x$ and TiSi_2 . Development of these solid-state reactions explains why the brittle $\text{Ti}_5\text{Si}_3\text{C}_x$ phase is no more present in the sub-layers covered by SiC. The texture difference between a Ti_3SiC_2 sub-layer located near the previously deposited SiC film and a Ti_3SiC_2 sub-layer located near the next SiC film (Fig. 8 and 9) evidences the difference between both mechanisms: mainly solid-gas ($\text{SiC-H}_2/\text{TiCl}_4$) reaction for the first one and solid-solid ($\text{Ti}_5\text{Si}_3\text{C}_x\text{-SiC}$) reaction for the second one.

At first sight, in the case of solid-gas reactions, this work seems to raise discrepancies between thermodynamic calculations and experimental results. The reasons for this discrepancies will be analyzed in the following by considering different cases: low R value (i) or high R value (ii) and for a high R value: thin coatings (iia) and thick coatings (iib).

When $R = 4$ (i), Fig. 1a shows that we should obtain pure Ti_3SiC_2 rather than the TiC obtained experimentally (Fig. 5). The previously calculated deposition diagram [11] showed that to obtain TiC at equilibrium, R should be less than 2.3 for a co-deposition with Ti_3SiC_2 and equal to about 0.5 for pure TiC growth. This first seeming discrepancy could originate from a mere shift between the R ratio used for calculation and the experimental ratio and more particularly by a shift between the ratio corresponding to the gaseous system H_2/TiCl_4 introduced in the CVD reactor and the actual ratio for H_2 and TiCl_4 molecules really reaching the SiC substrate surface where the reaction takes place. As H_2 is nearly one hundred times less dense than TiCl_4 gas, after convection through the reactor, the gas may be poorer in hydrogen at the bottom part of the hot area where the carbon disk substrates are set. Also, the diffusion rates of hydrogen across the boundary layer at the substrate surface could be different from the one of titanium chloride, which might be responsible for a change of the R ratio.

When $R = 35$ and when only thin layers are deposited by RCVD during short deposition times (iia), the precursor gas phase is in direct contact with uncovered SiC solid substrate. As

a gaseous phase is less dense than a solid phase, this case should correspond to a small quantity of TiCl_4 reacting with SiC , i.e. $n(\text{TiCl}_4) < n(\text{SiC})$. In that case, as long as SiC is still present at equilibrium, Ti_3SiC_2 should be co-deposited with TiSi_2 (Fig. 1b). Experimentally, if thin Ti_3SiC_2 layers could be actually obtained in these conditions, TiS_2 was never detected in thin coatings realized in less than 10 minutes (Fig. 14). Once again, if a decrease of the R ratio is admitted, the thermodynamic calculations that predict the growth of pure Ti_3SiC_2 by partial consumption of SiC when R is less or equal to 20 (and superior to 2.3) are in accordance with the experimental result.

Finally, for thick coatings prepared with a high R value (iib), after the formation of pure Ti_3SiC_2 , the growth of Ti_3SiC_2 and $\text{Ti}_5\text{Si}_3\text{C}_x$ is observed as predicted by the thermodynamic calculations for $n(\text{TiCl}_4) > n(\text{SiC})$ (Fig. 1b) and $R > 6.7$ [11]. This point can be achieved when the Ti_3SiC_2 sub-layer is thick enough ($\sim 1.5 \mu\text{m}$) to isolate the SiC substrate from the gaseous molecules, which results in the vanishing of SiC from the system at equilibrium according to thermodynamics. However, the simultaneous formation of both ternary compounds does not result from the expected co-deposition since the phases are not mixed in one layer but separated in two distinct continuous sub-layers. It is worth noting that, once a continuous reaction layer has formed at the substrate surface by RCVD, this layer acts as a diffusion barrier. Further reaction between the substrate and the gas phase can then only proceed by solid state volume diffusion through the barrier layer. Even if local equilibria still exist at the substrate/layer and layer/gas interfaces, chemical potential gradients take place in the barrier layer and the underlying substrate is no more in equilibrium with the gas phase [18,19]. Thus, the thermodynamic analysis presented in this paper and in reference [11] is actually no more valid when $t \gg t_{\text{crit}}$, and particularly it can no longer be used to account for the experimental results when $(\text{TiCl}_{4(g)}) \gg n(\text{SiC}_{(s)})$.

At this point, the diffusion path concept and solid state reaction-diffusion models [18-20] appear as the most appropriate tools to describe further development of the RCVD process. The parabolic curve presented in Fig. 6 for a low R value is thus typical of a diffusion mechanism. (The plateau observed for very long time deposition can be attributed to the development of pores in TiC by Kirkendall effect that end up by cutting off the diffusion path.) The introduction of inert markers should be useful in further work for better understanding of the growth of thick Ti-Si-C layers by RCVD.

Conclusion

The RCVD method allows a sub-micrometer SiC surface layer to be converted into Ti_3SiC_2 in a few minutes if a sufficient dilution of the titanium tetrachloride vapor in hydrogen is used to avoid the direct growth of TiC. These results accord with thermodynamics if a shift between the R ratio used for calculation and the experimental ratio is admitted. Hence, with periodic changes of the gases introduced in the CVD reactor, it is possible to deposit $(\text{SiC}/\text{Ti}_3\text{SiC}_2)_n$ multilayered coatings as long as short enough treatment times are used for the growth of each Ti_3SiC_2 thin sub-layer. For long deposition times, the RCVD treatment of SiC results in the formation of TiC and $\text{Ti}_5\text{Si}_3\text{C}_x$ additional sub-layers through solid state diffusion. The alternation of these thick coatings with SiC layers results in the further conversion of the additional brittle phases into new Ti_3SiC_2 sub-layers from solid state reactions that involve TiSi_2 as an intermediate phase.

References

- [1] M. W. Barsoum, T. El-Raghy, "Synthesis and characterization of a remarkable ceramic: Ti_3SiC_2 " J. Am. Ceram. Soc. 79(7) (1996) 1953.
- [2] J. M. Molina-Aldareguia, J. Emmerlich, J.-P. Palmquist, U. Jansson, L. Hultman "Kink formation around indents in laminated Ti_3SiC_2 thin films studied in the nanoscale", Scr. Mater. 49(2) (2003) 155.
- [3] J. Emmerlich, H. Högberg, S. Sasvári, P. O. Å. Persson, L. Hultman, J.-P. Palmquist, U. Jansson, J. M. Molina-Aldareguia, Z. Czigány "Growth of Ti_3SiC_2 thin films by elemental target magnetron sputtering" J. Appl. Phys. 96(9) (2004) 4817.
- [4] R. Wenzel, F. Goesmann, R. Schmid-Fetzer, "Diffusion barriers on titanium-based ohmic contact structures on SiC." High-Temperature Electronic Materials, Devices and Sensors Conference, San Diego, Feb. 22-27, 1998 159.
- [5] M. W. Barsoum, T. El-Raghy, C. J. Rawn, W. D. Porter, H. Wang, E. A. Payzant, C. R. Hubbard, "Thermal properties of Ti_3SiC_2 " J. Phys. Chem. Solids 60(4) (1999) 429.
- [6] J.-P. Palmquist, U. Jansson, T. Seppänen, P. O. Å. Persson, J. Birch, L. Hultman, P. Isberg "Magnetron sputtered epitaxial single-phase Ti_3SiC_2 thin films" Appl. Phys. Lett. 81(5) (2002) 835.
- [7] J. J. Nickl, K. K. Schweitzer, P. Luxenberg, "Gas-phase deposition in the titanium-silicon-carbon system" J. Less Common Met. 26(3) (1972) 335.
- [8] T. Goto, T. Hirai, "Chemically vapor deposited titanium silicon carbide (Ti_3SiC_2)" Mater. Res. Bull. 22(9) (1987) 1195.
- [9] E. Pickering, W. J. Lackey, S. Crain, "CVD of Ti_3SiC_2 " Chem. Vap. Deposition 6(6) (2000) 289.
- [10] C. Racault, F. Langlais, R. Naslain, Y. Kihn, "On the chemical vapor deposition of Ti_3SiC_2 from $TiCl_4$ - $SiCl_4$ - CH_4 - H_2 gas mixtures. Part II. An experimental approach" J. Mater. Sci. 29(15) (1994) 3941.
- [11] S. Jacques, H. Di-Murro, M.-P. Berthet, H. Vincent, "Pulsed reactive Chemical Vapor Deposition in the C-Ti-Si system from $H_2/TiCl_4/SiCl_4$ " Thin Solid Films, 478 (2005) 13.
- [12] J.C. Viala, N. Peillon, F. Bosselet, J. Bouix, "Phase equilibria at 1000°C in the Al-C-S-Ti quaternary system: An experimental approach" Mater. Sci. Eng., A 229(1-2) (1997) 95.
- [13] J. C. Schuster, "Design criteria and limitations for SiC-metal and Si_3N_4 -metal joints derived from phase diagram studies of the systems Si-C-metal and Si-N-metal." Ceram. Trans. 35 (1993) 43.

- [14] Ke Tang, Chang-an Wang, Yong Huang, Xingli Xu, "Analysis on preferred orientation and purity estimation of Ti_3SiC_2 " J. Alloys Compd 329 (2001) 136.
- [15] W. J. J. Wakelkamp, F. J. J. van Loo, R. Metselaar, "Phase relations in the Ti-Si-C system" J. Eur. Ceram. Soc. 8(3) (1991) 135.
- [16] C. Racault, F. Langlais, C. Bernard, "On the chemical vapour deposition of Ti_3SiC_2 from $TiCl_4$ - $SiCl_4$ - CH_4 - H_2 gas mixtures: Part I. A thermodynamic approach" J. Mater. Sci. 29(19) (1994) 5023.
- [17] Y. Du, J. C. Schuster, H. J. Seifert, F. Aldinger, "Experimental investigation and thermodynamic calculation of the titanium-silicon-carbon system" J. Am. Ceram. Soc. 83(1) (2000) 197.
- [18] J. S. Kirkaldy, L. C. Brown, "Diffusion behavior in ternary multiphase systems" Can. Metall. Q. 2(1) (1963) 89.
- [19] F. J. J. Van Loo, "Multiphase diffusion in binary and ternary solid state systems" Progr. Solid State Chem. 20 (1990) 47.
- [20] V. I. Dibkov "Growth kinetics of chemical compound layers", Cambridge Int. Sci. pub, Cambridge (UK), 1998

Legends

Fig. 1. Calculated quantities of solid species produced at equilibrium from $\{H_2/TiCl_4\}$ gaseous mixture reaction on 1 mole of SiC for $R = 4$ (a) and $R = 35$ (b) versus the quantity of $TiCl_4$ ($R = H_2/TiCl_4$, $1100^\circ C$, 5 kPa).

Fig. 2. SEM observation of $(S_{150}/T_{240})_1$ coating deposited with $R = 4$.

Fig. 3. EPMA of $(S_{150}/T_{240})_1$ coating deposited with $R = 4$.

Fig. 4. SEM observation of $(S_{20}/T_r)_4$ coating deposited with $t = 15, 25, 35$ and 45 minutes and with $R = 4$.

Fig. 5. BF TEM observation and SAED pattern (insert) of the fourth bi-layer (S_{20}/T_{45}) of $(S_{20}/T_r)_4$ coating $\{t' = 15', 25', 35'$ and $45'\}$ deposited with $R = 4$.

Fig. 6. Thicknesses of TiC layers deposited with $R = 4$ versus treatment durations.

Fig. 7. XRD pattern of $(S_{60}/T_{90})_3$ deposited with $R = 35$.

Fig. 8. SEM observation and EPMA of $(S_{60}/T_{90})_3$ deposited with $R = 35$.

Fig. 9. SEM observation of $(S_{30}/T_{30})_6$ coating deposited with $R = 35$.

Fig. 10. XRD pattern of $(S_{30}/T_{30})_6$ deposited with $R = 35$.

Fig. 11. BF TEM observation and SAED patterns (inserts) of sub-layer $n^\circ 5$ of $(S_{30}/T_{30})_6$ deposited with $R = 35$.

Fig. 12. TEM EDS analysis of Ti-Si-C sub-layer $n^\circ 2$ (a), sub-layer $n^\circ 5$ (b) and sub-layer $n^\circ 6$ (c) of $(S_{30}/T_{30})_6$ coating deposited with $R = 35$. (carbon concentration not represented)

Fig. 13. SEM observation of $(S_{10}/T_{10})_n$ (a) and $(S_3/T_3)_n$ (b) deposited with $R = 35$.

Fig. 14. XRD pattern of $(S_3/T_3)_n$ deposited with $R = 35$.

Figures

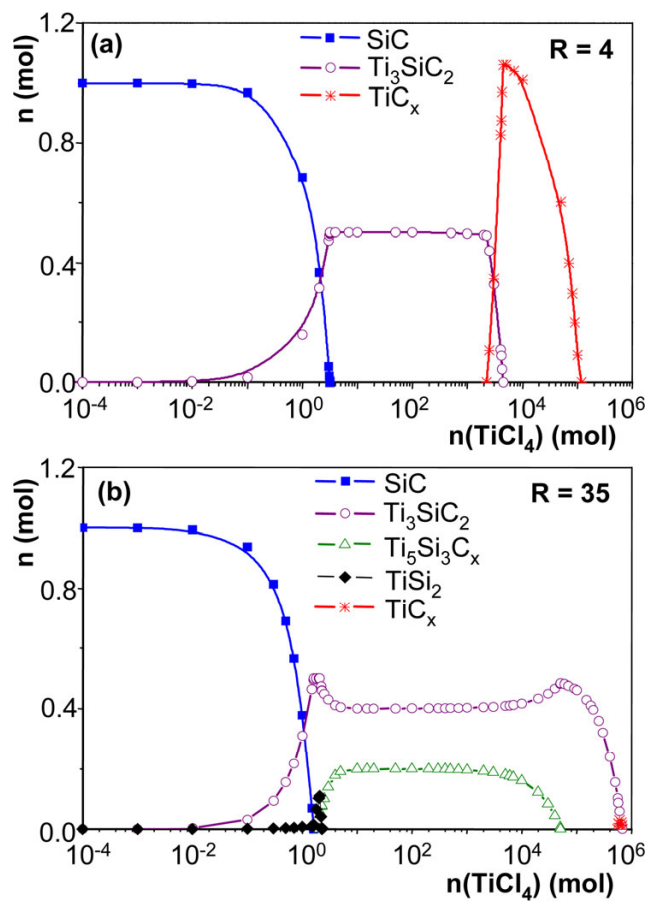


Fig. 1. Calculated quantities of solid species produced at equilibrium from $\{H_2/TiCl_4\}$ gaseous mixture reaction on 1 mole of SiC for $R = 4$ (a) and $R = 35$ (b) versus the quantity of TiCl₄ ($R = H_2/TiCl_4$, 1100°C, 5 kPa).

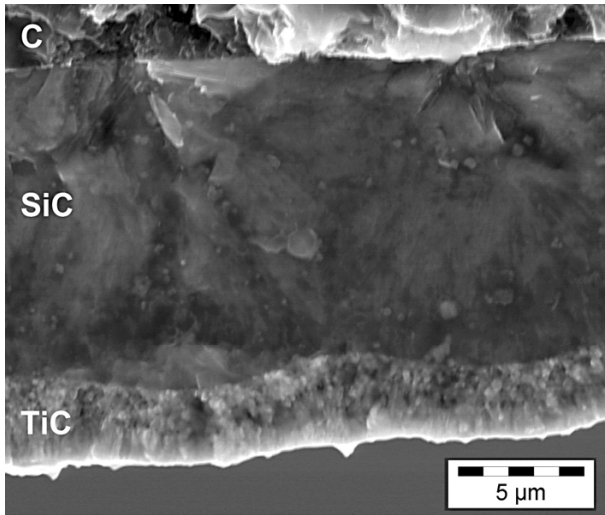


Fig. 2. SEM observation of $(S_{150}/T_{240})_1$ coating deposited with $R = 4$.

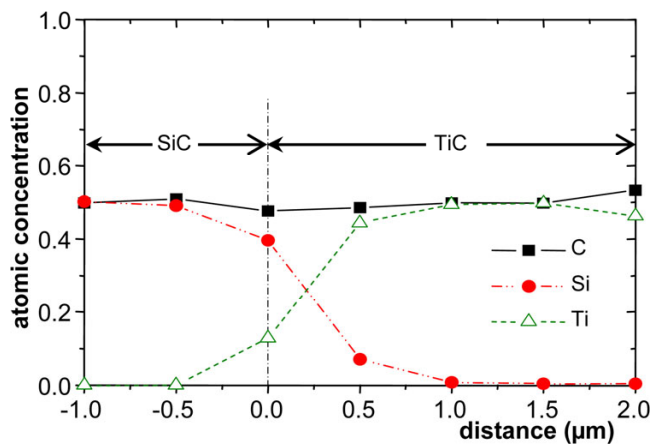


Fig. 3. EPMA of $(S_{150}/T_{240})_1$ coating deposited with $R = 4$.

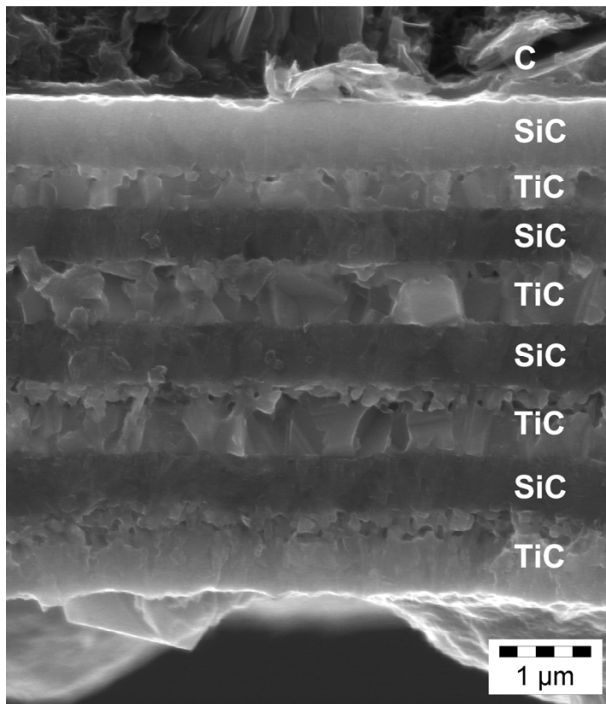


Fig. 4. SEM observation of $(S_{20'}/T_{r'})_4$ coating deposited with $t = 15, 25, 35$ and 45 minutes and with $R = 4$.

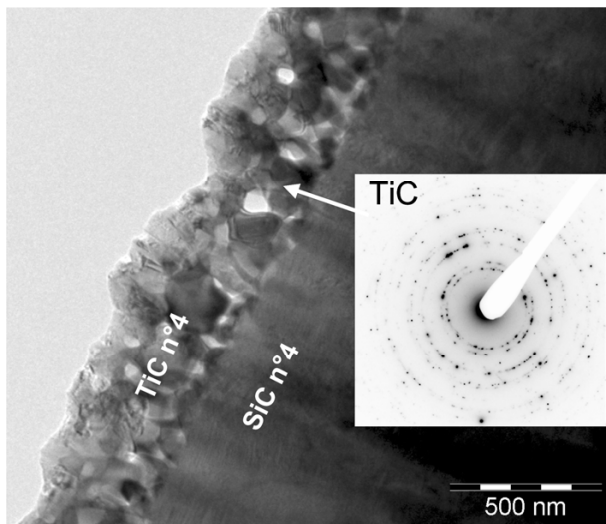


Fig. 5. BF TEM observation and SAED pattern (insert) of the fourth bi-layer $(S_{20'}/T_{45'})$ of $(S_{20'}/T_{r'})_4$ coating $\{t' = 15', 25', 35'$ and $45'\}$ deposited with $R = 4$.

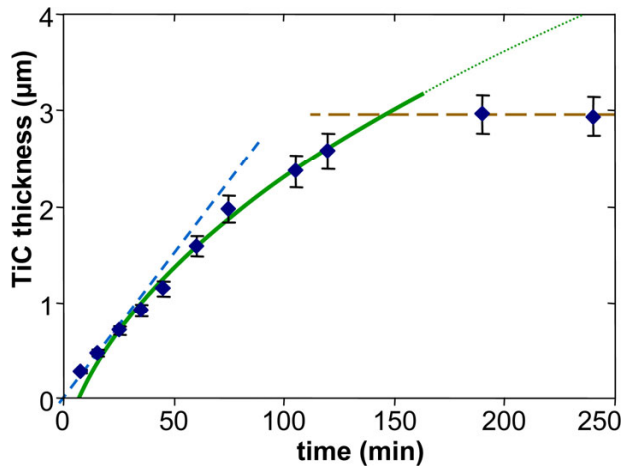


Fig. 6. Thicknesses of TiC layers deposited with $R = 4$ versus treatment durations.

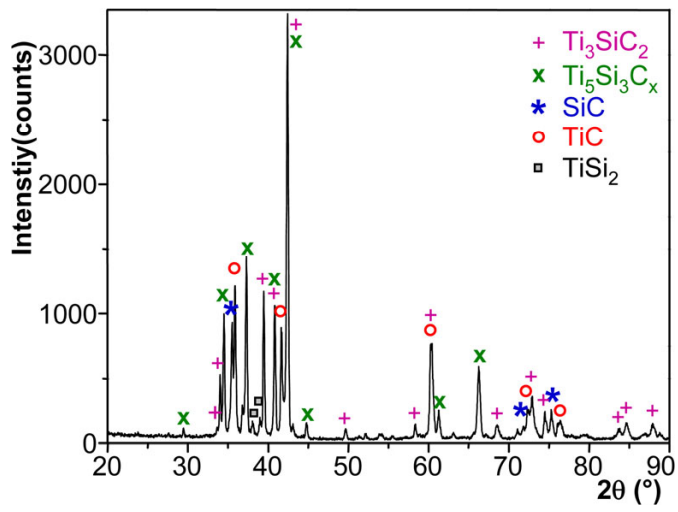


Fig. 7. XRD pattern of $(S_{60}/T_{90})_3$ deposited with $R = 35$.

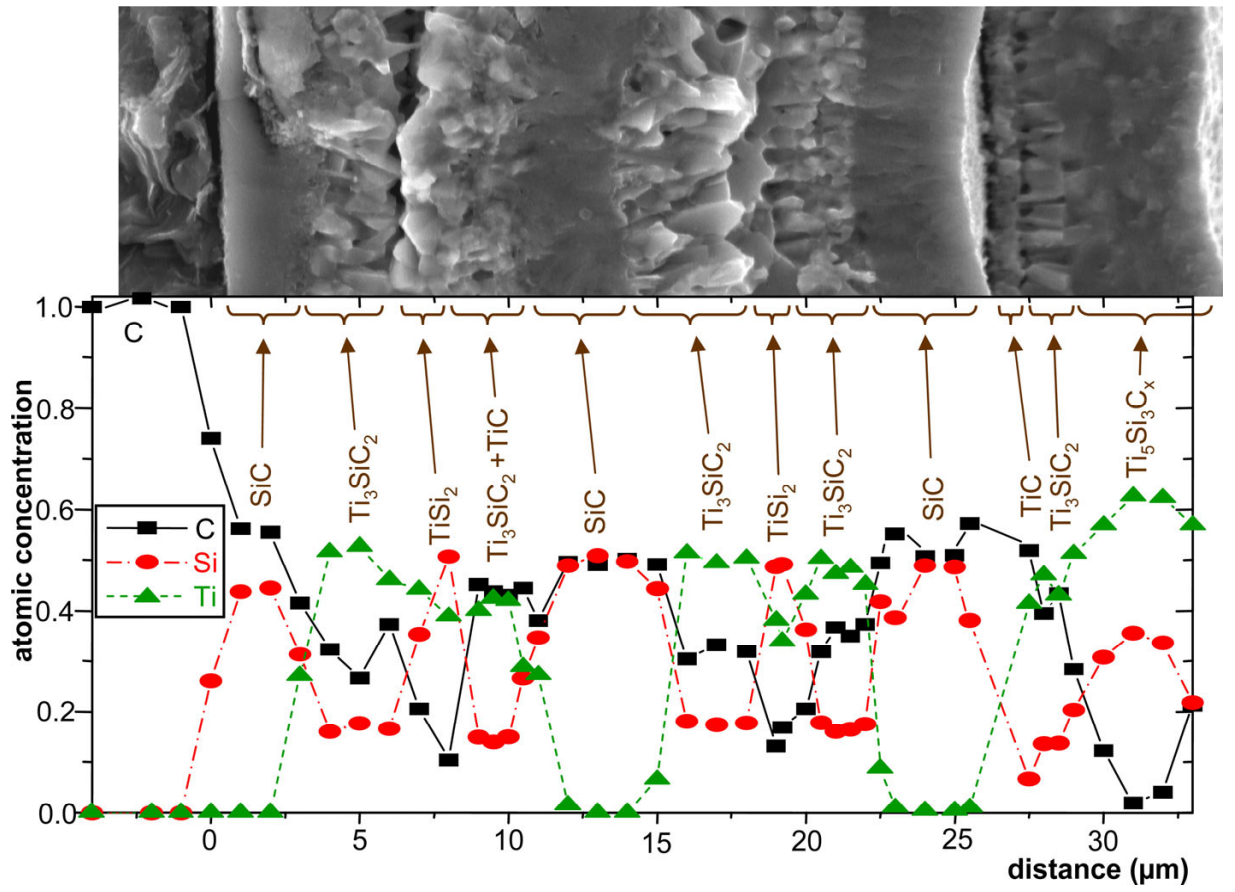


Fig. 8. SEM observation and EPMA of $(S_{60}/T_{90})_3$ deposited with $R = 35$.

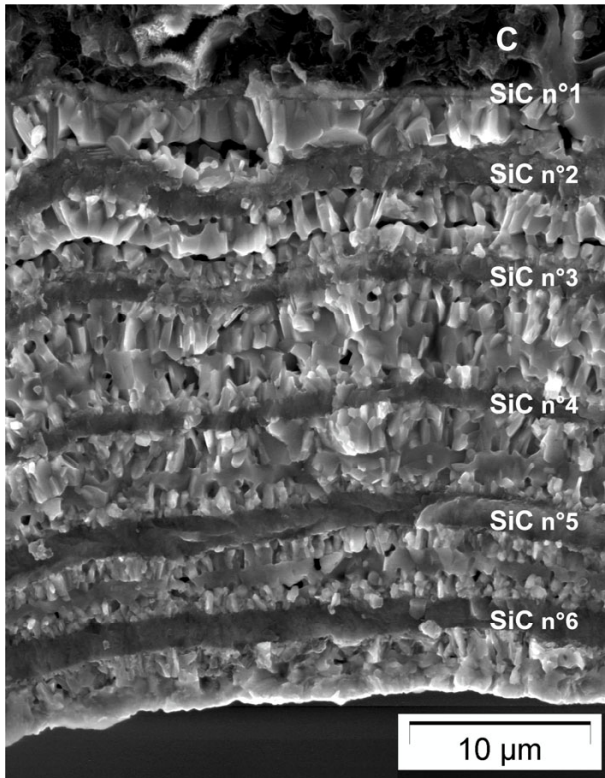


Fig. 9. SEM observation of $(S_{30}/T_{30})_6$ coating deposited with $R = 35$.

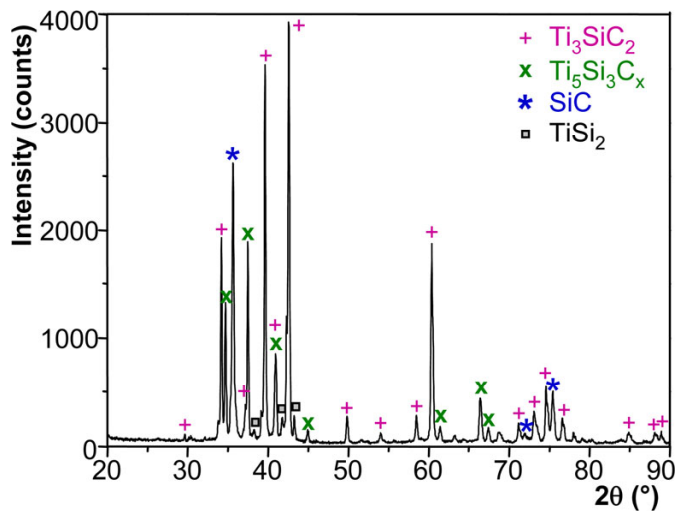


Fig. 10. XRD pattern of $(S_{30}/T_{30})_6$ deposited with $R = 35$.

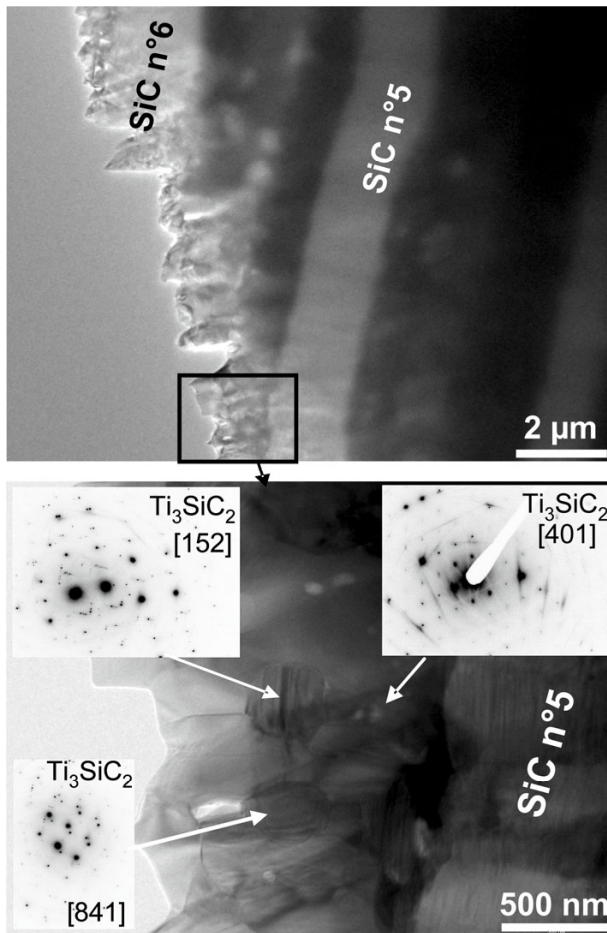


Fig. 11. BF TEM observation and SAED patterns (inserts) of sub-layer n°5 of $(S_{30}/T_{30})_6$ deposited with $R = 35$.

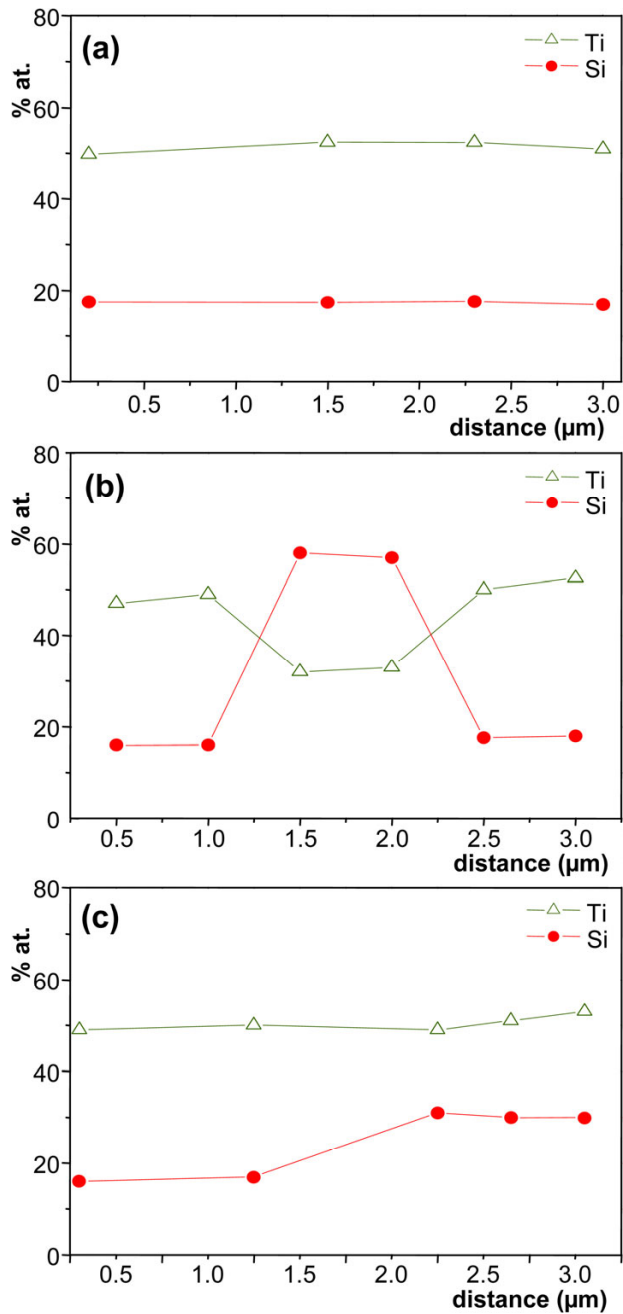


Fig. 12. TEM EDS analysis of Ti-Si-C sub-layer n° 2 (a), sub-layer n° 5 (b) and sub-layer n° 6 (c) of $(\text{S}_{30}/\text{T}_{30})_6$ coating deposited with $R = 35$. (carbon concentration not represented)

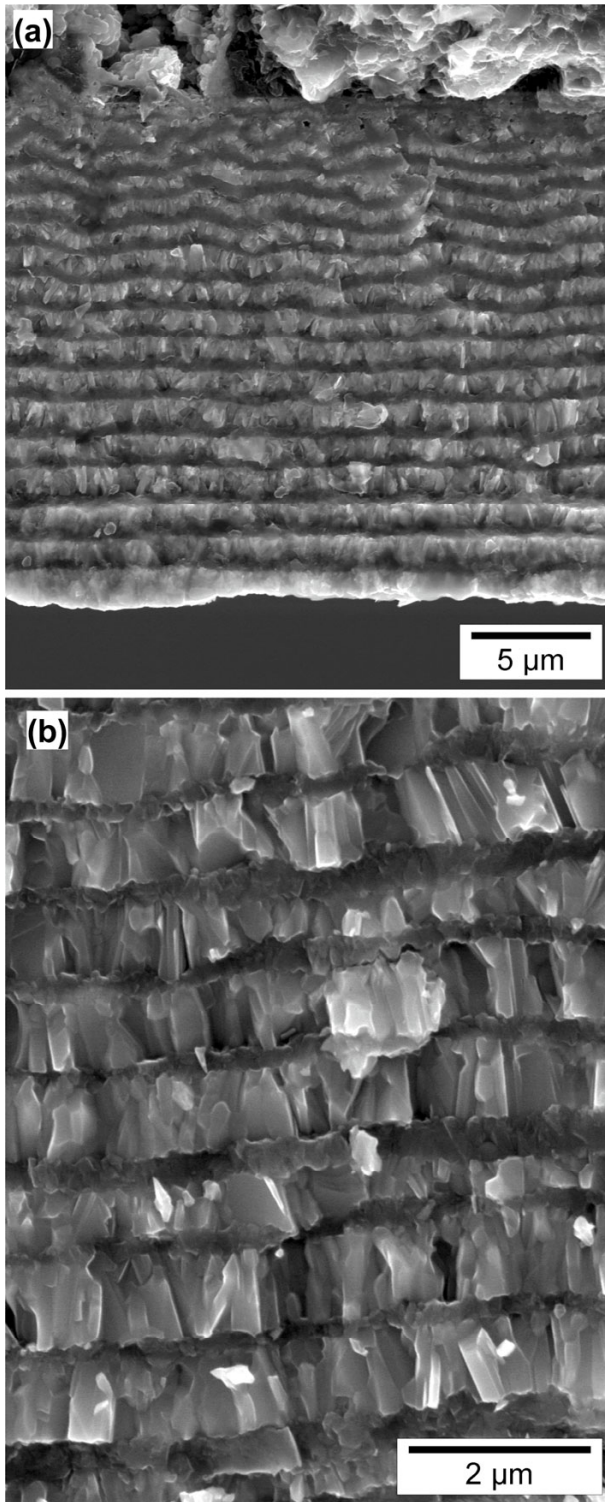


Fig. 13. SEM observation of $(S_{10}/T_{10})_n$ (a) and $(S_3/T_3)_n$ (b) deposited with $R = 35$.

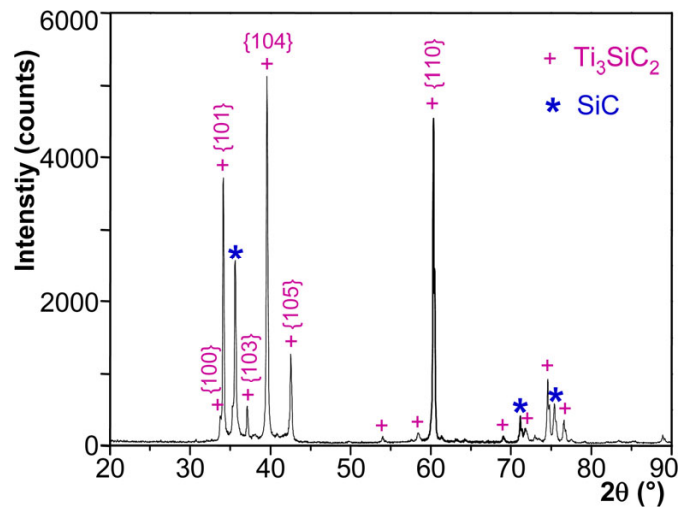


Fig. 14. XRD pattern of $(\text{S}_3/\text{T}_3)_n$ deposited with $R = 35$.